Helix Magic. Thermo-Driven Chiroptical Switching and Screw-Sense Inversion of Flexible Rod Helical Polysilylenes

Michiya Fujiki

Contribution from the NTT Basic Research Laboratories, 3-1 Wakamiya, Morinosato, Atsugi, Kanagawa 243-0198, Japan

Received October 29, 1999

Abstract: An ideal optically active helical chromophoric polymer comprising a flexible rodlike silicon main chain and enantiopure alkyl side chains, poly{(*S*)-3,7-dimethyloctyl-3-methylbutylsilylene}, underwent a thermo-driven helix−helix transition at −20 °C in isooctane. The transition characteristics, including transition temperature, transition width, the population of right- and left-handed helical motifs, global shape, and screw-pitch, were to be characterized quantitatively by spectroscopically analyzing circular dichroism (CD) and UV absorption characteristics. This is based on the unique property of the rodlike polymer in which the CD band completely matches the corresponding UV band profile at all temperatures. Moreover, fine controlling the contents and chirality of an additional chiral silylene unit incorporated in the copolymers allows free manipulation of the transition temperature in the range from −64 to +79 °C. Molecular mechanics calculation showed remarkable differences in the potential energy curve of the main chain torsion angle between flexible and rigid rodlike polysilylenes. These results and knowledge gained should assist in designing and controlling new types of helix−helix transition polymers directed to diverse screw-sense related properties and applications.

1. Introduction

The controlled synthesis and characterization of a pair of P (plus, right-handed) and M (minus, left-handed) screw-sense helical polymers are long-standing issues, covering a broad range of sciences and practical applications, such as biochemistry, polymer chemistry, supramolecular chemistry, analytical chemistry, and chiral separation column and chiral pharmaceutical technologies.[1,2] The widely accepted method to selectively obtain a helical polymer in one of the two possible screw forms is to change the chirality of the residues, repeating units, side chains, or initiators from dextro to levo or vice versa. Actually, for the respective oligo(dG-dC) duplex and protein, choice of the corresponding chiral amino acids and deoxyribose give ideal mirror-image chiral motifs.[3,4] An elegant alternative is helix−helix (PM) transition driven by an external stimulus, affording almost mirror-image helical motifs. Despite the finding almost three decades ago[5,6] by biochemists of this intriguing phenomenon in synthetic DNA, driven by change in salt concentration, and poly(*l*-aspartic acid ester)s, driven by a change in temperature, only calf thymus DNA[7] and several synthetic polymers[8−15] are known to undergo a PM transition driven by external stimuli so far. This is, perhaps, due to limited knowledge and understanding of the nature of PM transition characteristics.

Here the author reports an ideal synthetic polymer suitable for quantitatively studying thermo-responsive PM transition characteristics. The polymer is poly{(*S*)-3,7-dimethyloctyl-3-methylbutylsilylene} (**1**, Scheme 1), comprising a chromophoric rodlike helical silicon main chain bearing nonchromophoric enantiopure alkyl side chains. Polysilylenes are known to be soluble, chainlike semiconducting polymers with a chromophoric main chain.[16,17] It is noted that, among numbers of optically active polymers, only the rodlike helical main chain of polysilylenes gives a narrow exciton absorption band, due to the Siσ−Siσ* transition in the near-UV region, completely matching the corresponding circular dichroism (CD) and fluorescence band mirror image profiles.[18−20] The occurrence of the PM transition, therefore, was detected spectroscopically as an inversion of the CD band. Moreover, introduction of an additional chiral silylene moiety in the **1**-based copolymers permits the fine control of the PM transition over a wide range of temperature. These results indicate prospects for designing and controlling new types of PM transition polymers that may open the way to diverse screw-sense related applications, such

(1) Okamoto, Y.; Nakano, T. *Chem. Rev.* **1994**, *94*, 349−372.
(2) Farina, M. *Top. Stereochem.* **1987**, *17*, 1−111.
(3) Urata, H.; Shinohara, K.; Ogura E.; Ueda, Y.; Akagi, M. *J. Am. Chem. Soc.* **1991**, *113*, 8174−8175.
(4) Zawadzke, L. E.; Berg, J. M. *J. Am. Chem. Soc.* **1992**, *114*, 4002−4003.
(5) Pohl, F. M.; Jovin, T. M. *J. Mol. Biol*. **1972**, *67*, 375−396.
(6) Bradbury, E. M.; Carpenter, B. G.; Goldman, H. *Biopolymers* **1968**, *6*, 837−850.
(7) Mahadevan, S.; Palaniandavar, M. *Chem. Commun*. **1996**, 2547−2548.
(8) Toriumi, H.; Saso, N.; Yasumoto, Y.; Sasaki, S.; Uematsu, I. *Polym. J.* **1979**, *11*, 977−981.
(9) Watanabe, J.; Okamoto, S.; Satoh, K.; Sakajiri, K.; Furuya, H.; Abe, A. *Macromolecules* **1996**, *29*, 7084−7088.
(10) Okamoto, Y.; Nakano T.; Ono, E.; Hatada K. *Chem. Lett.* **1991**, 525−528.
(11) Maeda, K.; Okamoto, Y. *Macromolecules* **1999**, *32*, 974−980.
(12) Maxein, G.; Zentel, R. *Macromolecules* **1995**, *28*, 8438−8440.
(13) Bouman, M. M.; Meijer, E. W. *Adv. Mater*. **1995**, *7*, 385−387.
(14) Bidan, G.; Guillerez S.; Sorokin, V. *Adv. Mater*. **1996**, *8*, 157−160.
(15) Yashima, E.; Maeda, Y.; Okamoto, Y. *J. Am. Chem. Soc.* **1998**, *120*, 8895−8896.
(16) West, R. *J. Organomet. Chem*. **1986**, *300*, 327−346.
(17) Miller, R. D.; Michl, J. *Chem. Rev*. **1989**, *89*, 1359−1410.
(18) Fujiki, M.; Takigawa, H. Japanese Kokai Tokkyo Koho, JP 09,003,306 [97,003,306], 1997.
(19) Although further small-angle X-ray and neutron scattering (SAXS and SANS), and light scattering studies may be necessary to confirm whether the PM transition phenomenon is due to a single chain event, it is at present impossible because polysilylene solution is very dilute (10^{-4} mol/L) and the phenomenon occurs at low temperature.
(20) Fujiki, M.; Toyoda, S.; Yuan, C.-H.; Takigawa, H. *Chirality* **1998**, *10*, 667−675.

10.1021/ja9938581 CCC: $19.00
Published on Web 03/23/2000

Scheme 1. Chemical Structures of Polysilylene Homopolymers and Copolymers

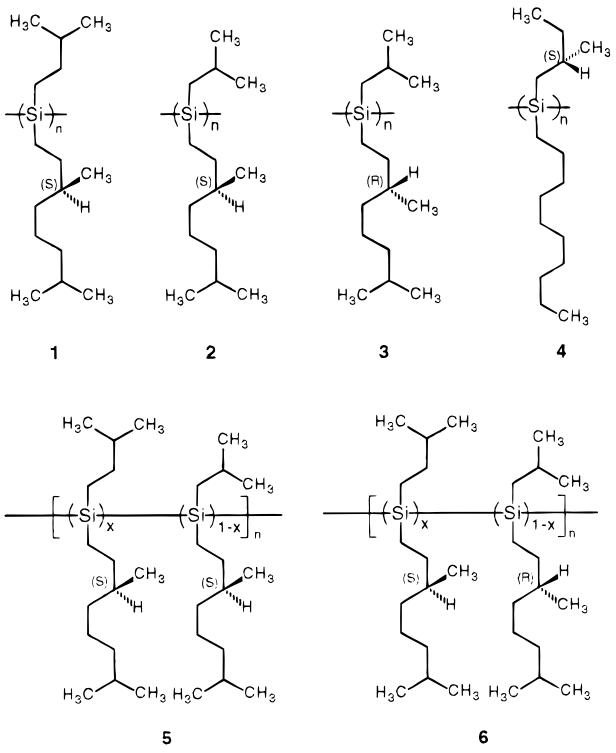

as a thermo-driven chiroptical switch and memory, and also a thermo-driven switching chiral separation column.

2. Results and Discussion

2-1. Helix−Helix Transition Polysilylene Homopolymer. Figures 1a and 1b compare the CD and UV absorption spectra of **1** at −40 and −5 °C and of poly{(*S*)-3,7-dimethyloctyl-2-methylpropylsilylene} (**2**, Scheme 1) at −82 and +80 °C in isooctane.[18] The positive-signed CD spectrum of **1**, with an extremum of 320 nm at −40 °C, is almost the inverse of the negative-signed CD spectrum, which has an extremum of 322 nm at −5 °C, over the whole 200 to 450 nm range. It is evident that there is a PM transition between the two temperatures for **1**, with helical motifs at −40 and −5 °C which are energetically and spectroscopically inequivalent. In contrast, **2** and its mirror-image poly{(*R*)-3,7-dimethyloctyl-2-methylpropylsilylene} (**3**, Scheme 1), which are derivatives of **1** with a β-branched achiral side chain, undergo no such inversion of the CD spectra in isooctane from −90 to +80 °C. Similarly, a change in temperature for poly{*n*-decyl-(*S*)-2-methylbutylsilylene} (**4**, Scheme 1) had almost no effect on the sign of the CD signal or the screw-sense.

Another possible explanation for the inversion of the 320-nm CD signal is due to aggregation and supercoiling. However, this can be excluded.[19] This is because, when a poor solvent was added to form an aggregate and/or a supercoil of an optically active rodlike helical polysilylene dissolved in good solvent, it has already been established that the spectral profile of a positive CD signal becomes bisignate with positive and negative bands and the intensities of these CD signals and the value of g_{abs} are enhanced by 1 to 2 orders of magnitude, indicating exciton coupling in a chiral arrangement between two polysilylene chains.[20]

Polymers **1**−**4** are thought to adopt almost rodlike 7_3-helical conformations (torsion angle of about 150° or 210°) in solution, since the λ_{max} values of these polymers near 320 nm are close

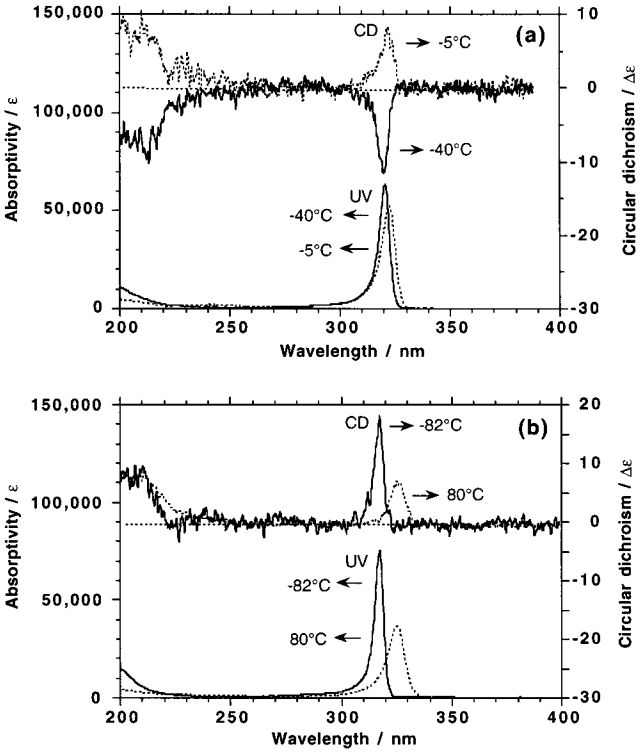

Figure 1. (a) CD and UV absorption spectra of **1** at −40 °C (solid line) and −5 °C (dotted line) in isooctane. (b) CD and UV absorption spectra of poly{(*S*)-3,7-dimethyloctyl-2-methylpropylsilylene} (**2**) at −82 °C (solid line) and +80 °C (dotted line) in isooctane. Either the ϵ or $\Delta\epsilon$ value was normalized as (Si-repeat-unit)$^{-1}$·dm^3·cm^{-1}. The weight-averaged molecular weight (M_w) of **1** was 1.6×10^6, and that of **2** was 4.2×10^4.

to that of poly(di-*n*-butylsilylene) which has a 7_3-helical form in the solid state.[17,21] Rodlike behavior is evidenced by the high viscosity index (α) of $[\eta] = \kappa \cdot M^{\alpha}$ in the Mark−Houwink−Sakurada plot, where $[\eta]$ is intrinsic viscosity and M is the absolute molecular weight, based on the universal calibration curve;[22] for **1** and **2** in $CHCl_3$ at 30 °C, the α values reached 1.11 ($\kappa = 2.7 \times 10^{-6}$ for $1.7 \times 10^4 < M < 6.3 \times 10^4$) and 1.29 ($\kappa = 4.7 \times 10^{-7}$ for $1.2 \times 10^4 < M < 4.8 \times 10^4$), respectively, and for **4** in tetrahydrofuran at 30 °C, the α value 1.35 ($\kappa = 1.9 \times 10^{-7}$ for $1 \times 10^4 < M < 2 \times 10^5$) was 1.35.[26] Nevertheless, rodlike **1** is much more flexible than rodlike **2** and **4**, according to the ^{29}Si NMR results for **1**, **2**, and **4**.

Figure 2 compares ^{29}Si NMR spectra of **1**, **2**, and **4** in $CDCl_3$ at 30 °C. Since **1**, **2**, and **4** have two different types of side chains attached to silicon backbone, they are essentially configurational stereoisomers, containing sequences such as isotactic, syndiotactic, atactic, and heterotactic. Surprisingly, both **1** and **2**, however, exhibit single ^{29}Si NMR signals near −25 to −23 ppm, perhaps suggesting a single configurational stereoisomer, isotactic or syndiotactic sequence. On the other hand, **4** contains a major ^{29}Si NMR signal at −22.2 ppm with a weak minor ^{29}Si NMR signal at −23.1 ppm, suggesting an almost single configurational stereoisomer but including a minor fraction of another type of configurational sequence in the same backbone.

It should be noted that there is a remarkable difference among **1**, **2**, and **4** in ^{29}Si NMR signal line width ($\Delta\nu_{1/2}$). The greater degree of flexibility of **1** compared to **2** and **4** is suggested by the narrower $\Delta\nu_{1/2}$: for **1**, $\Delta\nu_{1/2} = 29$ Hz at −25.3 ppm, while

(21) Fujiki, M. *J. Am. Chem. Soc.* **1994**, *116*, 6017−6018.
(22) Fujiki, M. *J. Am. Chem. Soc.* **1996**, *118*, 7424−7425.

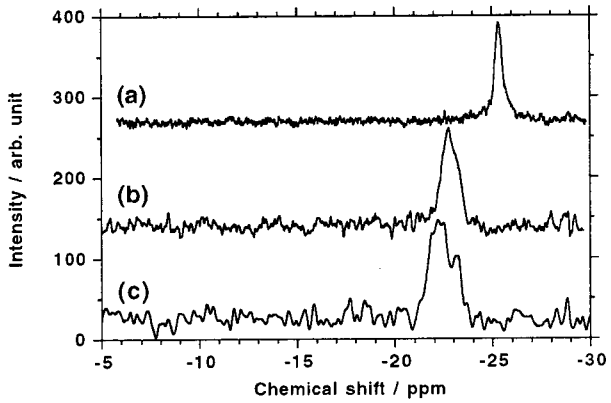

Figure 2. ^{29}Si NMR spectra of (a) **1**, (b) **2**, and (c) **4** in $CDCl_3$ at 30 °C. (See Table 1: **1**, fraction 2; **2**, fraction 2; and **4**, fraction 2.)

for **2**, $\Delta\nu_{1/2}$ = ca. 65 Hz at −22.7 ppm and for **4**, $\Delta\nu_{1/2}$ = ca. 90 Hz at −22.3 ppm.[21] Another noticeable difference among **1**, **2**, and **4** is their ^{29}Si NMR chemical shifts. The chemical shift of **1** is upfield compared to those of **2** and **3** by ca. 3 ppm, although the chemical shifts of **2** and **3** are very close to that of trans-planar poly(di-*n*-hexylsilane) in the ordered solid phase.[25] The downfield chemical shift of **2** and **3** is assumed to originate from elongation of the Si−Si bond length due to sterically hindered β-branched alkyl side chains. This is because the chemical shift of flexible rodlike helical **1** with less sterically hindered γ-branched alkyl side chains is very close to that of poly(di-*n*-hexylsilane) in the disordered solid phase. The significant difference in the degree of main chain rigidity is also supported by the results of molecular mechanics calculations for **1** and **2**, as described later.

Although the silicon backbones of homopolymer with two γ-branched side chains per repeat unit may undergo a PM transformation, either β- and γ-branched or β- and nonbranched side chains severely restrict any twisting of the main chain. Minute modification of the side chain structures thus definitively determines the possibility of the PM transition and its CD characteristics.

Figures 3a, 3b, and 3c show the temperature dependence of the CD and UV peak wavelengths and intensities of **1** and **2** in isooctane. As the temperature decreases from +80 to −82 °C, the CD and UV peak wavelengths of **1** and **2** linearly blueshift from ca. 325 to 318 nm, and the UV peak intensities (ϵ) of **1** and **2** monotonically increase from ca. 40000 to ca. 80000. The former is ascribed to a slight increase in screw-pitch, deviating from an ideal 7_3-helical structure.[24] The latter is due to a progressive increase in the radius of gyration of the main chain associated with an increase in effective conjugating main chain length, while **1** is likely to maintain its rodlike structure at those temperatures.[19] However, when the temperature changes from +80 to −82 °C, the $\Delta\epsilon$ value of **1** monotonically increases from ca. 3 at 80 °C to ca. 8 at −5 °C, but goes to zero abruptly at −20 °C, and then decreases to ca. −15 monotonically, while that of **2** monotonically increases from ca. 7 to ca. 18. It is emphasized that to quantitatively characterize the P- and M-helical populations of optically active polysilylenes, the

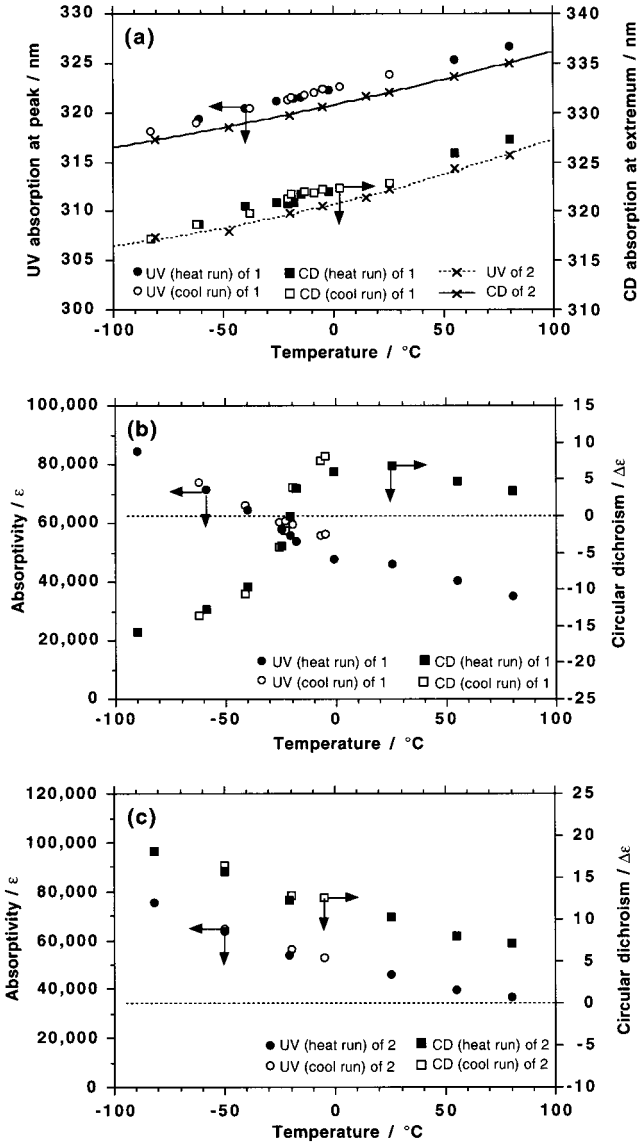

Figure 3. (a) Temperature dependence of **1** in isooctane: UV peak (filled circle for heating run and open circle for cooling run) and CD (filled square for heating run and open square for cooling run) wavelengths. Temperature dependence of **2** in isooctane: CD (dotted line with X) and UV peak (solid line with X). (b) Temperature dependence of **1** in isooctane: UV (filled circle for heating and open circle for cooling runs) and CD (filled square for heating and open square for cooling runs) peak intensities. (c) Temperature dependence of **2** in isooctane: UV (filled circle for heating run and open circle for cooling run) and CD (filled square for heating run and open square for cooling run) peak intensities. The cooling and heating rates in the cryostat measurement were 1−2° per minute (see ref 19).

dissymmetry ratio (g_{abs}) should be used instead of the $\Delta\epsilon$ value.[21,26,27]

Figure 4a compares the temperature dependence of the g_{abs} value of **1** for three samples of different molecular weight (M_w) and **2** with a thermally stable single-handed helix in isooctane. It is evident that in all three samples of **1** a steep PM transition clearly occurs at −20 °C (T_c), while **2** shows no such PM transition. These chiroptical properties are completely reversible in the heating and cooling runs. At T_c, mutual cancellation of positive and negative CD signals occurs, associated with an

(23) Recently, atomic force microscopy confirmed the rodlike form of **4** with a main chain length of up to 4000 nm, containing 150−800 nm long segments separated by kinks on sapphire. Ebihara, K.; Koshihara, S.; Yoshimoto, M.; Maeda, T.; Ohnishi, T.; Koinuma, H.; Fujiki, M. *Jpn. J. Appl. Phys.* **1997**, *36*, L1211−L1213.

(24) Teramae, H.; Takeda, K. *J. Am. Chem. Soc.* **1989**, *111*, 1281−1285.

(25) Schilling, F. C.; Lovinger, A. J.; Zeigler, J. M.; Davis, D. D.; Bovey, F. A. *Macromolecules* **1989**, *22*, 3055−3063.

(26) Fujiki, M. *Appl. Phys. Lett.* **1994**, *65*, 3251−3253.

(27) Dekkers, H. P. J. M. In *Circular Dichroism*; Nakanishi, K., Berova, N., Woody, R. W., Eds.; VCH: New York, NY, 1994; Chapter 6.

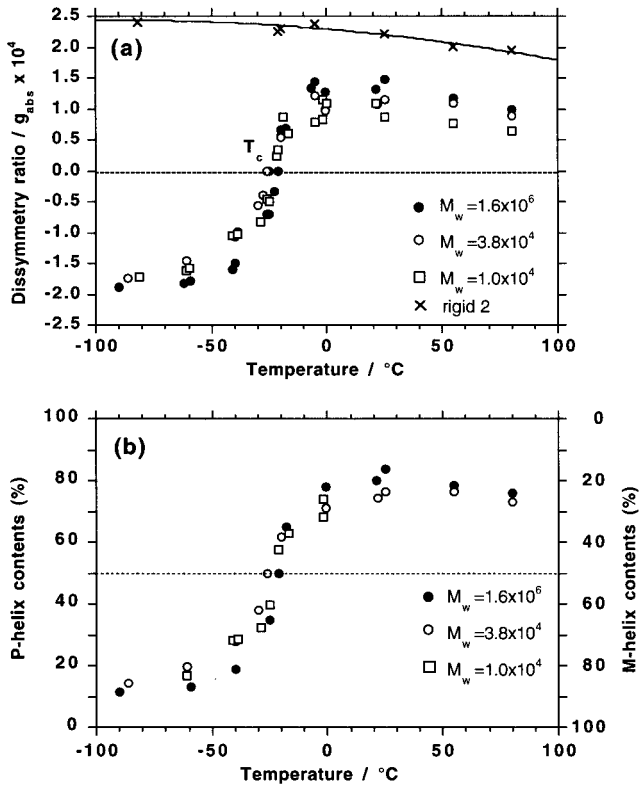

Figure 4. (a) Temperature dependence of the dissymmetry ratios (g_{abs}) of **1** with three different M_w samples and **2** with a thermally stable single-handed helix in isooctane. The values of M_w used were (i) 1.6×10^6 (filled circle), (ii) 3.8×10^4 (open circle), and (iii) 1.0×10^4 (open square) for **1** and 4.2×10^4 (x) for **2**. (See Table 1.) (b) Temperature dependence of P- and M-populations in **1** in isooctane with a calibration from the regression g_{abs} curve of **2**.

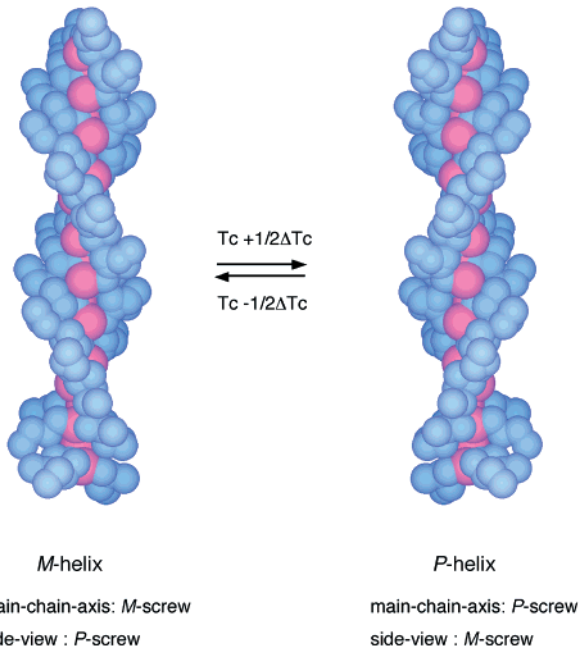

Figure 5. An illustration of the PM transition of the flexible rod polysilylene with P- and M-7_3 helical motif. The T_c means the temperature of the transition and ΔT_c refers to the temperature width of the transition. Red and blue colors refer to silicon and carbon atoms, respectively.

equal population of P- and M-helical motifs with the same photoexcitation energy. Although the origin of the PM transition is not understood clearly, a shortening of Si−Si bond length due to decrease in temperature is assumed to be directly responsible for the transition because there are no significant changes in the CD and UV absorption intensities and wavelengths just below and above T_c. For simplicity, we arbitrarily call the helical motif giving the positive CD band a P-helix, while the helical motif with the negative CD band is called an M-helix, since the relation between the screw-sense and the sign of the CD band is not clear.

To quantitatively discuss an ensemble averaged population of P- and M-motifs in helical polysilylenes, we compare the temperature dependence of the g_{abs} value in PM-active **1** with that of the second-order regression g_{abs} curve in PM-inactive **2** comprising a thermally stable P-helix. The population of P- and M-helices can be evaluated from the following simple equation, $P(\%) = 100(1 + g_{abs}(T)/g_{max}{}^{P}(T))/2$, and $M(\%) = 100 - P(\%)$, while $g_{abs}(T)$ and $g_{max}{}^{P}(T)$ are the observed g_{abs} values of **1** and **2** at a given temperature. It is assumed that the weak temperature dependence of the $g_{max}{}^{P}(T)$ value for **2** is due to an increase in the screw-pitch of the P-helix, rather than a minor formation of the M-helical motif.

Figure 4b replots the temperature dependence of the P- and M-populations in **1** with three different M_w samples in isooctane, calibrated from the second-order regression g_{abs} curve of **2**. It is clear that the P- and M-populations of **1** slightly depend on M_w; the high M_w fraction contains 12% P- and 88% M-motifs at −90 °C, while at +25 °C these values are 84% P- and 16% M-motifs. The medium and low M_w fractions contain 15% P- and 85% M-motifs at −90 °C, while at +25 °C these values are 76% P- and 24% M-motifs. In addition, the transition temperature width (ΔT_c) tends to broaden slightly as M_w decreases. Because the PM transition characteristics including T_c, ΔT_c, and populations of P- and M-motifs weakly depend on the molecular weight, segment lengths shorter than fifty silicon repeating units and two main chain end termini may determine the PM-transition characteristics.

Figure 5 illustrates schematically the PM transition of the flexible rod polysilylene with a right-handed or left-handed 7_3 helical motif. Thus, **1** is able to switch dynamically between P- and M-motifs at any temperature. CD measurement on a fast heating run (>1 °C per s) and the ^{29}Si NMR line width of **1** imply that the transition time near T_c was less than 1 s, and possibly less than 1 μs, although this cannot be confirmed without further temperature-jump experiments. Empirical knowledge and understanding of PM-transition and main chain flexibility of rodlike polysilylenes led us to believe that minute structural changes in the achiral alkyl pendants critically control the flexibility of the helical polysilylene and may modify the PM transition characteristics. To test this, we prepared a series of **1**-based copolymers (**5** and **6**).

2-2. Helix−Helix Transition Polysilylene Copolymers. Figures 6a and 6b compare the temperature dependence of the g_{abs} values and the populations of P (%) and M (%) of **5** (with 80% of **1** and 20% of **2**), **1**, and **6** (with 80% of **1** and 20% of **3**) in isooctane in the range −82 and +80 °C. It can be seen that, compared to the T_c of **1**, that of **5**, containing two identical (*S*)-chiral side chains per repeat unit, is lower by 16 °C, whereas that of **6**, containing different (*S*)- and (*R*)-chiral side chains per repeat unit, is higher by 16 °C. The CD spectral profile for the respective copolymers still matches the corresponding UV absorption spectrum at any temperature. However, introduction of moieties of **2** or **3** in the copolymers increases the ΔT_c value. Perhaps randomness of the two silylene repeating units in the copolymers and a distribution of the mean segment length near T_c may determine the ΔT_c value.

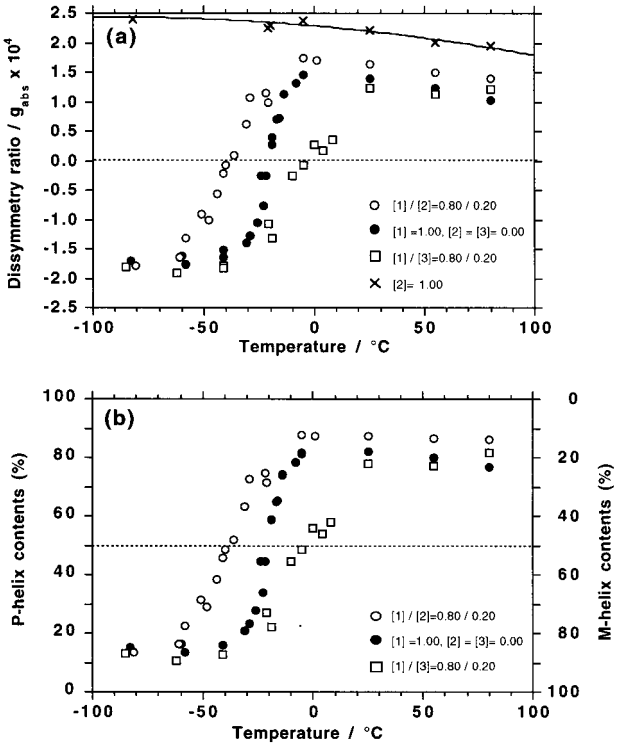

Figure 6. (a) Temperature dependence of the g_{abs} values of **5** (with 80% of **1** and 20% of **2**, $M_w = 5.0 \times 10^4$, open circle), **1** ($M_w = 3.8 \times 10^4$, filled circle), **6** (with 80% of **1**, 20% of **3**, $M_w = 4.8 \times 10^4$, open square), and **2** ($M_w = 4.2 \times 10^4$, X) in isooctane. (See Table 1.) (b) Temperature dependence of the populations of P (%) and M (%) of the **5**, **1**, and **6** samples in isooctane.

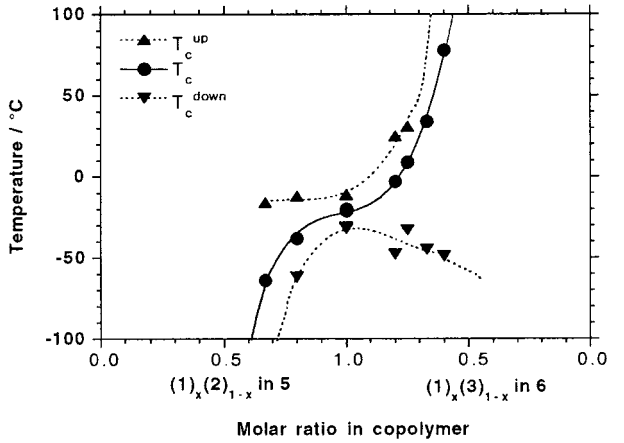

Figure 7. The values of T_c and ΔT_c as a function of molar fraction of **1** in **5**, and **1** in **6** in isooctane. The M_w values in all the copolymers ranged from 8.5×10^4 to 3.5×10^4, referenced to polystyrene standards. (See Table 1.)

Figure 7 plots the values of T_c and ΔT_c as a function of the molar fraction of **1** in **5**, and **1** in **6**. It can be seen more clearly that the T_c value can be continuously varied from −64 to +79 °C and the value of ΔT_c is nonlinearly broadened, as the molar fraction of **1** decreases, and that of **2** in **5** or **3** in **6** increases. Although a further mechanistic study is needed to clarify the real origin of the transition, as for the already well-studied cooperative helical response of semirigid poly(alkylisocyanate)s,[28] we now assume that the presence of two local free energy minimum potentials of the helical torsion angle and entropy term in the free energy stability are responsible for the transition. In addition, coexistence of P- and M-helical motifs in the same main chain at any temperature, even sufficiently low below T_c and sufficiently high above T_c, may be essential for the polymer to undergo the PM-transition, as shown in Figure 4b. This picture and idea will be supported from molecular mechanics calculations of their model oligomers.

(28) Green, M. M.; Peterson, N.; Sato, T.; Teramoto, A.; Cook, R.; Lifson, S. *Science* **1995**, *268*, 1860−1866.

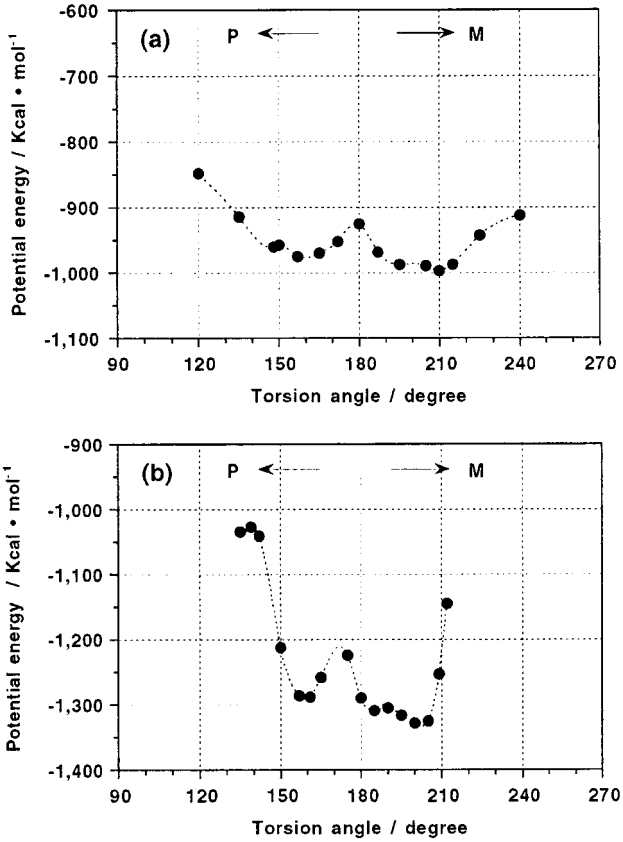

Figure 8. Molecular mechanics calculation. The Si−Si−Si−Si torsion angle dependence on the potential energy of (a) isotactic and (b) syndiotactic (*S*)-3,7-dimethyloctyl{3-methylbutyl}silylene 31-monomer units terminated with hydrogen (**7**).

2-3. Molecular Mechanics and Helix−Helix Transition Mechanism. Figures 8 and 9 show the Si−Si−Si−Si torsion angle dependence on the potential energy of (*S*)-3,7-dimethyloctyl{3-methylbutyl}silylene 31-monomer units terminated with hydrogen (**7**) and (*S*)-3,7-dimethyloctyl{2-methylpropyl}silylene 31-monomer units terminated with hydrogen (**8**) for their isotactic and syndiotactic stereoisomers, respectively (see Scheme 2). (See details of molecular mechanics calculation in the Experimental Section.)

From Figure 8, an isotactic **7** clearly shows a double well potential curve which means two local steric energy minima with almost enantiomeric helices at about 157° (P-helix) and 210° (M-helix) of torsion angles. The global minimum M-helical structure is slightly more stable than the corresponding P-helix by about 21 kcal/mol. This value corresponds to 0.67 kcal per Si repeating unit and 0.75 kcal per SiSiSiSi dihedral set. The barrier heights of the M- and P-screw-senses are 67 and 53 kcal, respectively. In other words, the barrier heights of the M- and P-helices are about 2.3 and 1.7 kcal per Si repeating unit and 2.6 and 1.9 kcal per SiSiSiSi dihedral set, respectively. The ratio of the barrier heights is only about 1.4. Surprisingly, a syndiotactic **7** also has a double well potential curve at about 160° (P-helix) and 200° (M-helix) torsion angles. The global minimum M-helical structure is slightly more stable than the corresponding P-helix by about 42 kcal/mol. This value is

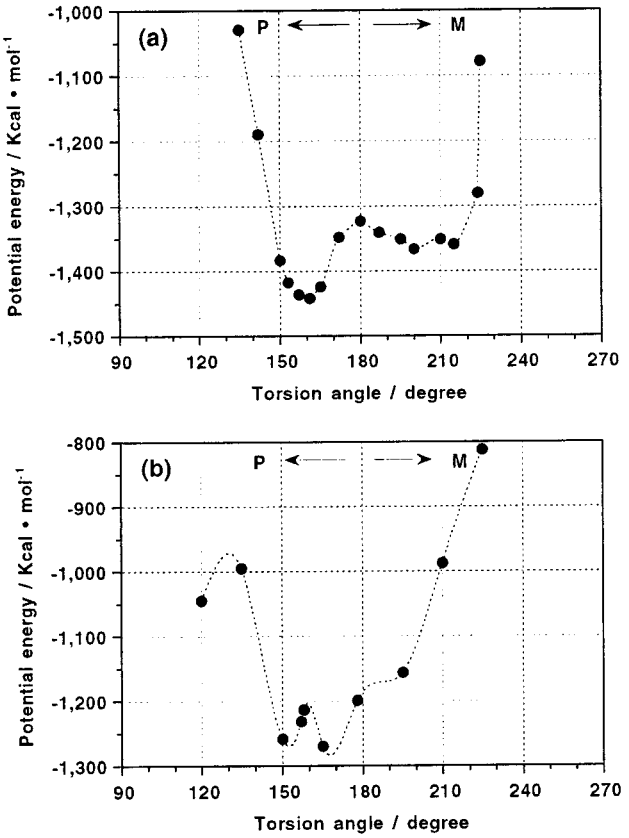

Figure 9. Molecular mechanics calculation. The Si−Si−Si−Si torsion angle dependence on the potential energy of (a) isotactic and (b) syndiotactic (*S*)-3,7-dimethyloctyl{2-methylpropyl}silylene 31-monomer units terminated with hydrogen (**8**).

Scheme 2. Isotactic and Syndiotactic Structures of Asymmetrically Substitued Dialkylpolysilylene, $(R_1R_2Si)_n$[a]

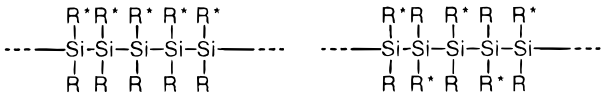

[a] See: Metanomski, W. V. *Compendium of Macromolecular Nomenclatue (IUPAC)*; Blackwell: Oxford, 1991; Chapter 2. This is identical to the case of isotactic polyethylidene.

evaluated to 1.3 kcal per Si repeating unit and 1.5 kcal per SiSiSiSi dihedral set. The barrier heights from the respective M- and P-screw-senses are 104 and 64 kcal, about 4.6 and 3.4 kcal per Si repeating unit, and 5.2 and 3.8 kcal per SiSiSiSi dihedral set. Thus, the calculation of **7** suggests that both pseudo-enantiomeric P- and M-helices are likely to stably coexist in the same main chain at any temperature, regardless of isotactic, syndiotactic, and perhaps even atactic sequences.

Contrarily, from Figure 9, an isotactic **8** shows an unclear double well potential curve having two local steric energy minima with enantiomeric helices at about 160° (P-helix) and 200° (M-helix) torsion angles. The P-helix is more stable compared to the corresponding M-helix by about 72 kcal/mol. This value suggests 2.3 kcal per Si repeating unit and 2.6 kcal per SiSiSiSi dihedral set. The barrier heights of the respective M- and P-screw-senses are 120 and 43 kcal, about 3.9 and 1.4 kcal per Si repeating unit, and 4.3 and 1.5 kcal per SiSiSiSi dihedral set. Because the ratio of the barrier heights reaches about 2.9, the P-helical **8** might be very stable, compared to the case of the isotactic **7**. A syndiotactic **8** has an almost single well potential curve at P-helix of around 160° of torsion angles. The P-helical structures of **8** and **2**, then, are considered to stably coexist at any temperature, regardless of tacticity.

From these calculations and CD measurements, we assume the relationship between helicity and the sign of the CD band and reached the conclusion that the P-screw-sense of polysilylene gives the positive-sign CD signal based on the following two reasons: (i) **2** showed positive-sign CD signals in the range from −80 to +80 °C, while its model **8** essentially adopts P-screw-sense at 0 K, and (ii) **1** showed negative-sign CD signals at lower temperature, while its model **7** adopts preferential M-screw-sense at 0 K.

To discuss the origin of the PM transition, we simply evaluate energy parameters between P- and M-helical states of **1** and **7**. Here, ΔG is the difference in free energy between P- and M-helical states. Similarly, ΔH and ΔS are the differences in enthalpy and entropy between P- and M-helical states, respectively.

$$\Delta G = G_P - G_M = \Delta H - T\Delta S = H_P - H_M - T(S_P - S_M) \quad (1)$$

$$\text{where } \Delta H = H_P - H_M, \Delta S = S_P - S_M \quad (2)$$

at T_c, $\Delta G = 0$, then

$$T_c = \Delta H/\Delta S \quad (3)$$

Since **1** has $T_c = 253$ K and its model **7** has $\Delta H = -0.67$ kcal per isotactic Si repeating unit, **1** and **7** have $\Delta S = -2.9$ cal·K^{-1} at T_c. Below T_c, since ΔG is negative, then M-screw is more stable than P-screw. Conversely, above T_c, P-screw is stable than M-screw because of positive ΔG. From the analysis, to achieve thermo-driven PM transition characteristics of polysilylene at 250 K, it seems essential that the polysilylene have a double well potential curve with P- and M-motifs, a small ΔH value, and a small potential barrier height per repeating unit. This corresponds to the values that $\Delta H/RT$ = ca. 1 and E_b/RT = ca. 6−8 at $T_c = 253$ K. The ΔS term is responsible for the inversion of the preferential screw-sense helical of polysilylene. This means that below T_c, M-helical polysilylene in a low entropy state may have a highly ordered packing structure of side chains, whereas above T_c, P-helical polysilylene in a high entropy state may take a disordered arrangement of side chains. Schematic helical structure models of the P- and M-helical **1** below and above a PM transition temperature are illustrated in Figure 10. Perhaps copolymerization may suitably control the degree of order and disordered states of P- and M-helical polysilylene.

2-4. Perspectives. If we were able to design these parameters (ΔH, ΔS, and E_b) of an optically active helical polymer for a given system, we might obtain a new type of PM transition polymer directed to diverse screw-sense related properties with functionality at the desired conditions including T_c, solvents, pressure, and additives. Here the T_c in the field of switching applications may be called a threshold temperature or a gate temperature.

It has been reported recently that several synthetic optically active polymers undergo chiroptical switching by photoisomerization, changes in temperature, pH, and solvent polarity, cooling rates of films, and additions of chiral organic substances and organic acids.[8−15] A few chromophoric chiral small molecules

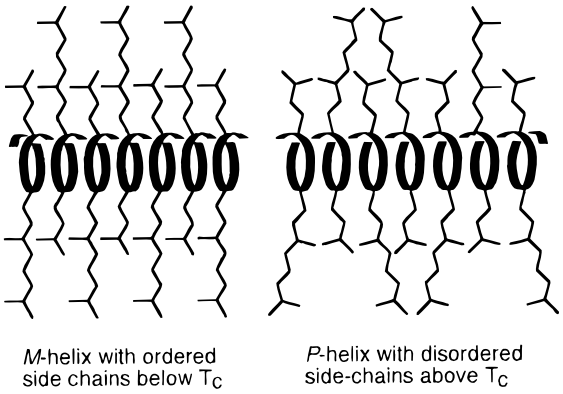

Figure 10. Schematic helical structure models of P- and M-helical **1** below and above a PM transition temperature.

also exhibit chiroptical switching with a PM transformation triggered by unpolarized and circularly polarized light photoisomerization.[29]

Controlled PM-transition polysilylenes able to switch between bistable chiroptical states with a thermal threshold may be very promising as chiroptical photonics materials suitable for the recently developed GaN laser diode (LD) emitting at 380−420 nm,[30] since bistable chiral photonics materials have recently received much interest in information and display technologies.[31−33] For example, alloys consisting of rare-earth and transition metals are now utilized as magnetooptical erasable recording media of chiroptical devices, although the media need both near-infrared LD and external magnetic fields. Ferroelectric liquid crystals with a surface-stabilized chiral smectic C phase have also been applied in spatial light modulators, image processing, photonic switching, and hologram devices by controlling polarized light and electric fields.[32,33] If there were an all-optical processing chiroptical material suitable for the GaN LD, a simpler chiroptical switch or high-density chiroptical storage device might be achieved. In the chiroptical device systems, a linearly or circularly polarized LD may switch between two chiroptical states with high-power heat and low-power photon modes. On the basis of understanding and knowledge of the controlled PM-transition polysilylenes demonstrated here, in the future, further appropriate chemical modification should allow us to develop new types of chiroptical photonics polymers with light and electric- and magnetic-field thresholds.

3. Conclusion

It was found that an ideal optically active helical polysilylene comprising a flexible rodlike main chain, poly{(*S*)-3,7-dimethyloctyl-3-methylbutylsilylene}, underwent a thermo-driven PM transition at −20 °C in dilute isooctane. Such transition characteristics as transition temperature, transition width, the population of P- and M-helical motifs, global shape, and screw-pitch were characterized spectroscopically using the CD and UV absorption characteristics of isolated polysilylene itself, not those of aggregation and/or supercoiling modes. This results from the unique property of the molecularly dispersed rodlike polysilylene in which the CD band profile completely matches the corresponding UV band profile at any temperature. In addition, controlling the contents and chirality of additional chiral silylene moieties, (*S*)-3,7-dimethyloctyl-2-methylpropylsilylene and (*R*)-3,7-dimethyloctyl-2-methylpropylsilylene, incorporated in the poly{(*S*)-3,7-dimethyloctyl-3-methylbutylsilylene}-based copolymers allowed fine-tuning of the transition temperature in the range from −64 to +79 °C. Molecular mechanics calculation indicated remarkable differences in the potential energy curve of the main chain torsion angle between the flexible and rigid rodlike polysilylenes. These results and knowledge encourage us in designing new types of desired PM transition polymers directed to diverse screw-sense-inversion related properties and applications.

4. Experimental Section

4-1. Apparatus. All CD and UV absorption spectra were recorded simultaneously on a JASCO J-720 spectropolarimeter equipped with a liquid nitrogen-controlled quartz cell with path length of 5 mm in a cryostat, ranging from 23 to −90 °C, and a Peltier-controlled quartz cell with path length of 10 mm, ranging from 60 to −10 °C. This temperature range ensures that isooctane is sufficiently fluid because the melting and boiling points of isooctane are −100 and 100 °C, respectively. Scanning conditions were as follows: a scanning rate of 50 nm per min, bandwidth of 1 nm, response time of 1 s, and double or single accumulations. Solution temperature in the cryostat was monitored by directly immersing a thermocouple into the solution, while solution temperature in the Peltier-controlled cell was considered to be the same as the aluminum block cell housing. The sample concentration was 2×10^{-5} (Si-repeat-unit)$^{-1}$ dm^{-3} for UV and CD measurements. ^{13}C (75.43 MHz) and ^{29}Si (59.59 MHz) NMR spectra were taken in $CDCl_3$ at 30 °C with a Varian Unity 300 NMR spectrometer using tetramethylsilane as an internal standard. Optical rotation at the Na-D line was measured with a JASCO DIP-370 polarimeter using a quartz cell with a path length of 10 mm at room temperature (24 °C). The weight-average molecular weight (M_w) and number-average molecular weight of polymers (M_n) were evaluated using gel permeation chromatography (Shimadzu A10 instruments, Shodex KF806M as a column, and HPLC-grade tetrahydrofuran as eluent at 30 °C), based on a calibration with polystyrene standards.

The viscosity−molecular weight measurement of polysilylenes was achieved and analyzed at the Toray Research Center (Shiga, Japan) using a Waters 1500 GPC apparatus with a Viscotec H502a viscometer. (see: Kinugawa, A. *The TRC News* **1994**, *13*, 27.)

4-2. Materials. The desired substituted dichlorosilane monomers were prepared by the condensation of the corresponding (*S*)-3,7-dimethyloctyl, (*R*)-3,7-dimethyloctyl, and (*S*)-2-methylbutyl Grignard reagent with the corresponding alkyltrichlorosilanes. A typical synthetic procedure of the dichlorosilane monomer, *(S)*-3,7-dimethyloctyl-3-methylbutyldichlorosilane (**11**), is shown in Scheme 2. 3-Methylbutyltrichlorosilane (**10**) was obtained by coupling 41 g (0.20 mol) of tetrachlorosilane (Shin-etsu) with Grignard reagent of 76.3 g (0.505 mol) of 3-methylbutylbromide (**9**) (Aldrich). Yield 57 g (57%; bp 68−72 °C/18 mmHg). ^{29}Si NMR: 13.56 ppm. ^{13}C NMR: 21.88, 22.15, 29.78, 30.90 ppm.

The dichlorosilane **11** was obtained by slowly adding Grignard reagent (**8**) obtained from 33 g (0.15 mol) of (*S*)-3,7-dimethyloctylbromide (**7**) (Chemical Soft, Kyoto, Japan) to 41 g (0.20 mol) of **10** in dry diethyl ether (Kanto) at room temperature. Filtration of the reaction mixture and vacuum distillation of filtrate afforded pure **11** in 62% yields. Bp 122−127 °C/1.5 mmHg. ^{29}Si NMR: 34.67 ppm. ^{13}C NMR: 17.35, 17.88, 19.10, 21.97, 22.62, 22.71, 24.73, 27.97, 29.12, 30.17, 31.15, 34.78, 36.46, 39.30 ppm. $[\alpha]^{24}_D$ +1.61° (neat).

The other monomer data are as follows. (*S*)-3,7-Dimethyloctyl-2-methylpropyl-dichlorosilane (**12**): yield 56%. Bp 104−105 °C/0.5 mmHg. ^{29}Si NMR: 33.34 ppm. ^{13}C NMR: 18.434, 19.092, 22.613, 22.704, 24.199, 24.722, 25.602, 27.964, 29.163, 30.313, 34.784, 36.453, 39.294 ppm. $[\alpha]^{24}_D$ −1.61° (neat);

(29) Huck, N. P. M.; Jager, W. F.; de Lange, B.; Feringa, B. L. *Science* **1996**, *273*, 1686−1688.
(30) Nakamura, S.; Senoh, M.; Nagahama, S.; Iwasa, N.; Yamada, T.; Matsushita, T.; Kiyoku, H.; Sugimoto, Y. *Jpn. J. Appl. Phys.* **1996**, *35*, L74−L76.
(31) Emmelius, M.; Pawlowski, G.; Vollmann, H. W. *Angew. Chem., Int. Ed. Engl.* **1989**, *28*, 1445−1471.
(32) Moddel, G.; Johnson, K. M.; Li, W.; Rice, R. A.; Pagano-Stauffer, L. A.; Handschy, M. A. *Appl. Phys. Lett.* **1989**, *55*, 537−539.
(33) Masatoshi, S.; Takeda, M.; Fukushima, S.; Kurokawa, T. *Appl. Opt.* **1998**, *37*, 7523−7531.

Scheme 3. Synthetic Scheme of Polysilylene **1**

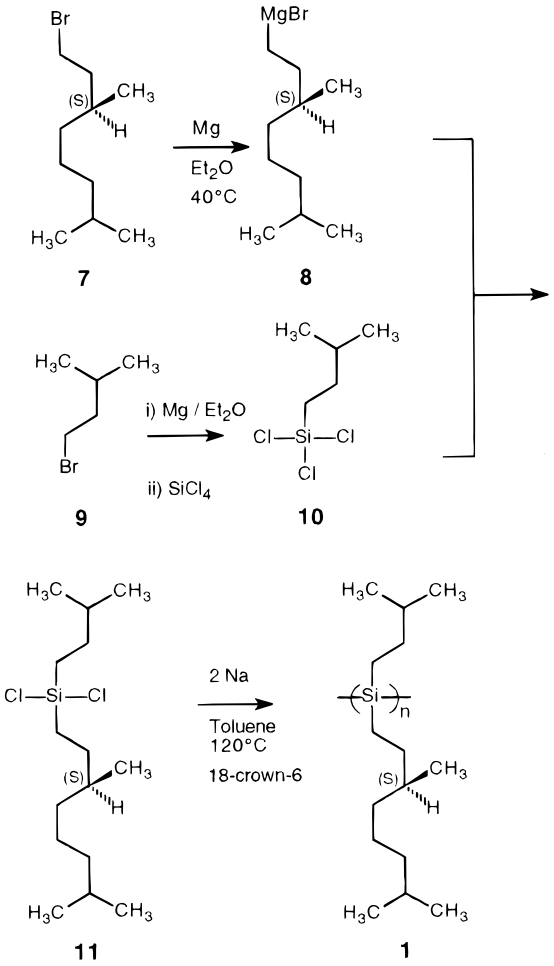

(*R*)-3,7-Dimethyloctyl-2-methylpropyldichlorosilane (**9**): yield 42%. Bp 86−92 °C/0.45 mmHg. ^{29}Si NMR: 33.22 ppm. ^{13}C NMR:18.37, 19.04, 22.56, 22.66, 24.140, 24.67, 25.55, 27.91, 29.140, 30.25, 34.73, 36.40, 39.24 ppm. $[\alpha]^{24}_{D}$ +1.76° (neat). (*S*)-2-Methylbutyl-*n*-decyldichlorosilane (13): yield 42%. Bp 119−121 °C/0.40 mmHg. ^{29}Si NMR: 33.19 ppm. ^{13}C NMR: 11.22,14.12, 21.33, 21.84, 22.45, 22.71, 28.08, 29.15, 29.34, 29.48, 29.63, 30.24, 31.93, 32.37, 32.52 ppm. $[\alpha]^{24}_{D}$ +7.64° (neat).

The purified dichlorosilanes were polymerized according to the conventional Wurtz-type condensation. The typical synthetic procedure of **1** is described as follows. To a mixture of 10 mL of dry toluene (Kanto), 0.80 g (0.035 mol) of sodium lump (Wako), and 0.06 g (0.23 mmol) of 18-crown-6 (Wako) was added 4.0 g (0.014 mol) of **11** dropwise in an argon atmosphere. The mixture was stirred slowly at 110 °C. After 2 h, 300 mL of dry toluene was added to reduce solution viscosity and stirring continued for a further 30 min. The hot reaction mixture was passed immediately through a 5-μm PTFE filter (Sumitomo Electric, Fluoropore) under argon gas pressure. To the colorless clear filtrate were added 2-propanol, ethanol, and methanol carefully as poor solvents. Several portions of white precipitates were collected by centrifugation (Kubota) and dried at 120 °C in a vacuum overnight. Two or three molecular weight fractions were obtained as white solids. The yields and some properties of polysilylenes **1**−**6** obtained in this work are summarized in Table 1.

Table 1. Characterization Data for Polysilylenes **1**−**6**

polysilylenes	ratio of copolymer	fraction	M_w	M_n	M_w/M_n	yield, %
1		1	1630000	1060000	1.53	16
		2	38000	20000	1.90	16
		3	10000	3790	2.64	4
2		1	3890000	2580000	1.51	33
		2	42300	23500	1.80	12
		3	6520	4940	1.32	2
3		1	7400000	4230000	1.75	3
		2	87600	41300	2.12	9
		3	28700	17900	1.60	8
4		1	5330000	4120000	1.29	4
		2	117000	37000	3.16	18
5	[1]/[2] = 0.67/0.33	1	3280000	1790000	1.84	3
		2	19600	41300	2.11	3
	[1]/[2] = 0.80/0.20	1	1840000	1010000	1.82	18
		2	49700	26400	1.88	9
6	[1]/[3] = 0.80/0.20	1	5970000	3700000	1.61	28
		2	48700	26600	1.83	12
	[1]/[3] = 0.75/0.25	1	5260000	3500000	1.50	24
		2	72100	25400	2.83	8
	[1]/[3] = 0.67/0.33	1	4850000	2940000	1.65	18
		2	40700	21600	1.88	8
	[1]/[3] = 0.60/0.40	1	4850000	2940000	1.65	6
		2	40700	21600	1.88	8

4-3. Molecular Mechanics Calculation. Molecular mechanics calculation was achieved using the Molecular Simulation Inc., Discover 3 module, Ver. 4.00, on Silicon Graphics Indigo II XZ based on standard default parameters with a Si−Si bond length of 2.34 Å and a Si−Si−Si bond angle of 111° using the MSI pcff force field. For this calculation, the MSI built-in function of simple-minimize and simple-dynamics was used with setup parameters which include 1.00 of the final convergency and 1000 iterations for minimization and temperature of 300 K for the dynamics.

Acknowledgment. The author thanks Hiromi Tamoto-Takigawa for CD, UV, and GPC measurements. Drs. Masao Morita, Hideaki Takayanagi, and Noriyuki Hatakenaka did much to encourage this work. Dr. Julian R. Koe and Hiroshi Nakashima are thanked for many fruitful discussions. Profs. Yoshihisa Inoue, Akio Teramoto, Takahiro Sato, Junji Watanabe, and Mark M. Green are acknowledged for fruitful discussions. This work was supported by CREST (Core Research for Evolutional Science and Technology) of JST (Japan Science and Technology Corporation).

JA9938581